Dynamic Modelling, Experimental Validation and Simulation of a Virtual District Heating Network

Loïc Giraud, Roland Bavière, Cédric Paulus, Mathieu Vallée, Jean-François Robin

Univ. Grenoble Alpes, INES, F-73375 Le Bourget du Lac, France
CEA, LITEN, F-38054 Grenoble, France, roland.baviere@cea.fr

Abstract:

District heating networks are expanding in France, thanks to their ability to reduce carbon dioxide emissions. Designing efficient control strategies for district heating network is one of the main challenges to achieve this goal. In this paper, we show how dynamic modelling, experimental validation and simulation of a district heating network can be combined to develop efficient control strategies. We first report on the development and validation of a modelling tool devoted to dynamic simulation of district heating system. We describe the models of the main components (heat only boiler, pump, pipe and substation) and we detail some of the experimental validation we have conducted. Several physical/numerical formulations are tested to select the best candidate in terms of accuracy and computational cost. Secondly, we introduce the simulation of a virtual district heating network designed after the district heating network of Grenoble, France. Two supply temperature control strategies are evaluated on the virtual network, showing that the advanced strategy reduces the distribution losses by an amount of 10 % compared to a fixed heating curve based on the outdoor temperature.

Keywords:

District heating network, Dynamic modelling, Supply temperature control strategy, Modelica.

1. Introduction

District heating systems are generally considered to deliver 6 % of the total heat demand in France. This figure is relatively low compared to the situation in northern European countries such as Denmark where more than 60 % of the heat demand is provided by such systems [1]. Due to environmental issues, such as the necessity in reduction of carbon dioxide emissions, the French government has recently decided to further develop district heating networks. According to [2], the amount of energy delivered in France by district heating should experience a growth rate of 300 % between 2007 and 2020. As a consequence, France is currently experiencing the construction of many small district heating networks while larger well-established systems continue their extension. Moreover, district heating control strategies are progressively modernized in order to reduce thermal distribution losses and improve the share of renewable and recovery energies.

Advanced district heating control strategies have first been studied in northern European countries along with the development of simulation capabilities [3–5]. In France, researches in this domain have started more recently [6]. In the recent years, new results have been obtained in the field of efficient physical modelling [7,8] and operational optimization [9]. Our work aims at pursuing these studies by developing computationally efficient and accurate dynamic simulation capabilities in order to propose and evaluate advanced control strategies.

The purpose of this paper is to show how accurate modelling of a district heating network can be used as a basis to develop efficient control strategies. Section 2 first describes the district heating component modelling approach that we have developed. Since the experimental validation of such models is an important issue, the validation process applied for the substation model is entirely described in section 2.6. In section 3, we describe the optimization of a temperature control strategy in a virtual district heating network, designed to reproduce the behavior of a small part of the district heating network in Grenoble, France. Consumers are simulated using actual heat load profiles observed in the Grenoble main district heating system. Two supply temperature control

strategies, a standard and an optimized strategy, are compared in order to show the potential of energy savings.

2. Modelling and experimental validation of component models

2.1. Simulation platform

The beginning of the present research program in January 2014 was devoted to the selection of an appropriate simulation platform, for instance able to host flexible model development. We have carried comparative studies of various candidates and the details of this analysis can be found in [10]. This work has led us to the conclusion that the equation-based object-oriented language Modelica [11] with the simulation platform Dymola [12,13] was the most adapted tool for our application. All the models reported in the present paper have therefore been programmed using the Modelica language.

2.2. Generalities on the component models

In order to build a virtual district heating network, the models of its elementary components must first be defined. In this section, simple and generic models of a heat only boiler, circulation pumps, thermally insulated pipes and substations are described.

In the present study, only liquid water is considered as the heat carrier fluid. In order to limit computational costs, the fluid is considered incompressible and non-expandable. Thus, for each component model, the mass balance is expressed as in (1).

$$\dot{m}_{in} + \dot{m}_{out} = 0 \quad (1)$$

Pressure waves propagate through a hydraulic network at a velocity exceeding 1000 m/s. Their travelling time seldom exceed one minute in a district heating system and can therefore be ignored in the present work. Thus, the dynamic term in the momentum balance expressed for each component model can be neglected for our application.

2.3. Heat only boiler

Since modelling the detailed internal behavior of a heat only boiler is out of the scope of the present study, we propose a very simplified and generic model. In this model, the mass and momentum balance equations are (1) and (2). The energy equation (see (3)) results from a simplified heat balance written for the fluid and solid parts. C' represents the solid thermal inertia of the boiler. The global heat transfer coefficient UA between the fluid and the external environment is supposed constant. The source term S is determined as in (4) where $\Delta T_{f,nom}$, $\Delta T_{ext,nom}$ and ΔT_{err} are constant parameters. For this study, the ΔT_{err} parameter was chosen equal to 0.01 K. This ensures that the outlet fluid temperature remains very close from the set point (i.e. $T_{out} - T_{set} \sim 0$).

$$P_{in} = P_{out} \quad (2)$$

$$\left(\rho_f V_f c_{p_f} + C'\right)\frac{dT}{dt} = \dot{m} c_{p_f}(T_{in} - T_{out}) - UA(T_{out} - T_{ext}) + S \quad (3)$$

$$S = \dot{m} c_{p_f} \Delta T_{f,nom} \frac{T_{out} - T_{set}}{\Delta T_{err}} + UA \Delta T_{ext,nom} \frac{T_{out} - T_{set}}{\Delta T_{err}} \quad (4)$$

2.4. Pump

In district heating, the pressure difference between the supply and return network is usually controlled by the operators to adapt the production to the heat demand. The simplified pump model is therefore composed of a mass balance equation as in (1), a momentum balance equation where the pressure difference matches the set point ΔP_{set} (5) and an energy balance equation where the pump efficiency is assumed to be 1 (see (6)).

$$P_{out} = P_{in} + \Delta P_{set} \quad (5)$$

$$\dot{m}(h_{out} - h_{in}) = \frac{\dot{m}}{\rho_f}\Delta P_{set} \quad (6)$$

2.5. Pipes

Thermal energy is distributed from district heating production plants to consumers by means of a collection of pipes, namely the supply network. Each pipe is essentially composed of a steel tube and a cylindrical thermal insulation layer. After delivering its energy to consumers, the heat carrier fluid is recycled by the production plant using the return network. In most district heating systems, the supply and return networks are identical.

Heat transportation through the network occurs at a velocity typically ranging from 0.05 m/s to approximately 2 m/s and over distances of a few to several tens of kilometers. This may give rise to a several hours delay before a temperature step initiated at a production plant reaches far end consumers. An advanced controller for the supply temperature of a district heating production plant must therefore encompass anticipation and temperature prognosis capabilities. Moreover, in order to build a physically relevant virtual district heating network, the temperature transportation time must be correctly accounted for. This is the main reason that led our research group to define a distribution pipe model representative of the temperature transportation dynamics. The developed model uses (1) and (7) to express mass and momentum balances. In (7), f is the fanning friction factor determined for nominal flow conditions (typically $v \sim 1$ m/s) thanks to the Swamee-Jain correlation [14]. Moreover, (7) is linearized in the region corresponding to the laminar regime.

$$P_{in} = P_{out} - 2f\frac{L}{D}\rho_f v|v| \quad (7)$$

The energy balance equation is derived according to the method of characteristics [15]. In a first step, the heat capacity of the steel tube is not taken into account. Since the fluid properties are supposed constant, the partial derivative equation expressing the energy balance of the heat carrier fluid is expressed as in (8):

$$\frac{\partial T}{\partial t} + v\frac{\partial T}{\partial x} = \frac{\dot{Q}_{losses}}{\rho_f V_f c_{pf}} \quad (8)$$

This expression is integrated along a fluid's particle path line, namely a characteristic curve [15], where (9) is verified:

$$\frac{dT}{dt} = \frac{\partial T}{\partial t} + v\frac{\partial T}{\partial x} \quad (9)$$

Combining (8) and (9) leads to the first order differential equation (10):

$$\frac{dT}{dt} = \frac{-Kdx(T_f - T_{ext})}{\rho_f V_f c_{pf}} \quad (10)$$

This last equation can be natively integrated within a Modelica based computer program [11] or integrated analytically as in (11),

$$T^*_{out}(t) = (T_{in}(t-\tau) - T_{ext})e^{-\frac{K\tau}{\rho_f A_f c_{pf}}} + T_{ext}, \quad (11)$$

where $T_{in}(t-\tau)$ represents the pipe inlet temperature at the past instant $t - \tau$. The transportation time, named τ, is determined using (12) where L is the length of the pipe:

$$\int_{t-\tau}^{t} v(s)ds = L \quad (12)$$

The relation between $T^*_{out}(t)$ and $T_{out}(t)$, respectively the outlet pipe temperatures without and with considering the heat stored in the steel tube is finally determined using (13). Equation (13) is obtained by assuming that the heat capacity of the whole tube is gathered at the outlet of the pipe and that the fluid and tube temperature are supposed equal.

$$\rho_a A_a L c_{p_a}\frac{dT_{out}}{dt} = \dot{m}c_{p_f}(T_{out} - T^*_{out}) \quad (13)$$

The modelling approach presented here is related to the « node method » detailed in the Danish scientific literature on district heating [3–5,16]. In order to validate our model, we compared its results to an analytical solution representing the response to a temperature step at the inlet of an

adiabatic steel tube. We also performed cross-comparisons to a finite volume model developed by our research group and as well as to several models reported in [16]. Finally, we compared the numerical predictions of the present model to available experimental data reported from the Vilnius district heating network [17]. All results showed that our model is a good compromise to perform accurate yet low computational cost simulations for our application. Due to space limitations, the results of these comparisons cannot be detailed here and will be left for a future publication.

2.6. Substations

2.6.1. Description

The heat transported throughout a district heating network is delivered to consumers by the mean of a substation. A substation is generally composed of a heat exchanger, a control valve positioned on the primary side and a PI controller used to control the secondary output temperature (see Fig. 1 a)). The substation models that we describe and compare in this section contribute to simulations covering time periods ranging from days to months. The detailed dynamics of the PI controller is then of minor importance for such simulations. The proposed models therefore consider an idealized behavior for the controller where the secondary output temperature always matches the set point value. As a consequence, the primary mass flow rate is entirely governed by the heat demand and does not depend on the local pressure difference between the primary supply and return lines. This last feature results in lower computational costs compared to components introducing hydraulic coupling between the supply and return lines (e.g. a by-pass). However, the valve opening computation considers the local pressure difference between the supply and return networks and relies on the Modelica incompressible valve model derived from [18]. The correspondence between the secondary heat demand and the primary mass flow rate is determined by means of a heat exchanger model which is described hereafter.

In this section, different heat exchanger models are proposed and evaluated in order to determine the best compromise between numerical accuracy and computational costs. The input and outputs of these models are schematically represented in Fig. 1 b) respectively using green and red colored fonts. We recall that $T_{out,s}$ is known since it is supposed equal to the set point value.

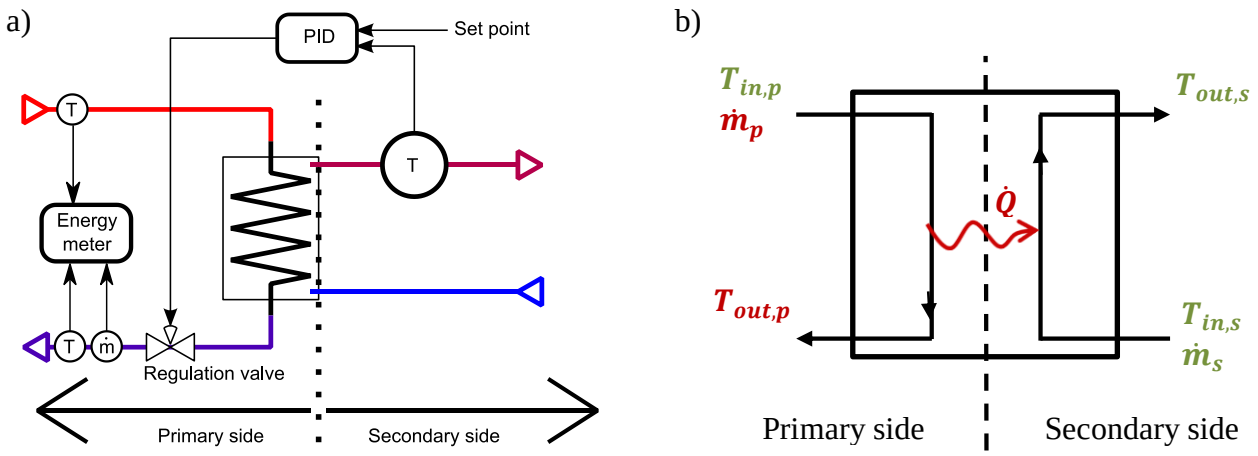

Fig. 1. Schematic representation of: a) a substation and b) a substation model

Each heat exchanger model is composed of 3 unknowns. The three corresponding equations are:

- 1 static energy balance equation respectively for the primary and secondary sides:

$$\dot{Q} = \dot{m}_p c_p \left(T_{in,p} - T_{out,p}\right) \quad (14)$$

$$\dot{Q} = \dot{m}_s c_p \left(T_{out,s} - T_{in,s}\right) \quad (15)$$

- 1 equation expressing the primary outlet temperature $T_{out,p}$ as a function of the other variables. Several modelling assumptions can be made for this expression.

2.6.1.1. ESM_0 model

The simplest model, namely ESM_0 (for Explicit Substation Model), that we propose for evaluation relies on a constant temperature approach assumption, as in (16),

$$T_{out,p} = T_{in,s} + k_1, \tag{16}$$

where k_1 is a fixed parameter that must be tuned for each case. This model has been proposed in [3] and is available in the TERMIS district energy network simulation platform [19]. One disadvantage of this method is that $T_{out,p}$ can lie outside of the physically acceptable range defined by:

$$T_{in,s} < T_{out,p} < T_{in,p} \tag{17}$$

2.6.1.2. ESM_1 model

To overcome the aforementioned difficulty, we propose the ESM_1 model defined by (18),

$$T_{out,p} = \alpha T_{in,p} + (1-\alpha) T_{in,s} \quad \text{with } 0 < \alpha < 1, \tag{18}$$

where α is a constant tunable parameter. Equation (18) is also used in ESM_2 and ESM_3 and LMTD models but α is then variable.

2.6.1.3. ESM_2 model

To reflect, in a simplified way, the variations of α with respect to the operating conditions of the heat exchanger, we assume in model ESM_2 that the primary and secondary mass flow-rates are identical. Relying on classical heat exchanger calculations (see [20]), this assumption leads for α to (19),

$$\alpha = \frac{\dot{Q}}{UA\left(T_{in,p} - T_{in,s}\right)}, \tag{19}$$

where UA, the global heat transfer coefficient, is a constant tunable parameter.

2.6.1.4. LMTD and ESM_3 models

According to the LMTD (Log Mean Temperature Difference) formulation [20], the exact dependency of α on operational conditions is the following equation:

$$\alpha = \frac{T_{in,p} - T_{out,s}}{T_{in,p} - T_{in,s}} \exp\left(-\frac{UA}{c_p \dot{m}_s}\left(\frac{\dot{m}_s}{\dot{m}_p} - 1\right)\right) \tag{20}$$

The UA parameter represents the global heat transfer coefficient. It is expressed as in (21) where the thermal resistance in the solid region is considered negligible. The dependency of UA on the mass flow-rates reflects the effect of the Reynolds number on the fluid/solid heat transfer coefficients on both the primary and secondary sides. Such a formulation is rather classical [3,21].

$$UA = \frac{k}{\dot{m}_p^{-q} + \dot{m}_s^{-q}} \tag{21}$$

Expressions (20) and (21) form the two parameters, namely k and q, LMTD model which is accurate but nonlinear and implicit. The computation of the LMTD model thus requires the use of an iterative method which can be numerically expensive. It is therefore meaningful to search for an approximate method relying on an explicit formulation.

We have established the ESM_3 model by searching an explicit formulation for the $\dot{m}_p$ term appearing in the mass flow-rate ratio in (20) and in the UA model in (21). Relying on the analysis of experimental temperature data taken from instrumented district heating substations, we propose the following explicit correlation between $\dot{m}_p$ and the inputs of the model:

$$\begin{aligned} &\dot{m}_s \geq \dot{m}_p: \qquad \epsilon = \epsilon_s = \frac{\dot{Q}}{\dot{m}_s c_p \left(T_{in,p} - T_{in,s}\right)} = c * \left(\frac{\dot{m}_s}{\dot{m}_p}\right)^{-b} \\ &\dot{m}_s < \dot{m}_p: \qquad \epsilon = \epsilon_p = \frac{\dot{Q}}{\dot{m}_p c_p \left(T_{in,p} - T_{in,s}\right)} = c * \left(\frac{\dot{m}_s}{\dot{m}_p}\right)^{b} \end{aligned} \tag{22}$$

The left hand-side of (22) is called the primary and secondary efficiency of the heat exchanger. It is defined as the ratio between the actual and the maximal possible exchanged thermal power. Due to the fact that b is a positive constant, the efficiency of the exchanger decreases as the ratio $\dot{m}_s/\dot{m}_p$ becomes increasingly remote from one. Four parameters must be determined to use the ESM3 model, namely b, c, k and q.

Table 1 summarizes the assumptions and formulation of the 5 heat exchanger models evaluated in the present work.

Table 1. Summary of the tested heat exchanger (substation) models

<table>
<tr><th>ESM_0</th><th>ESM_1</th><th>ESM_2</th><th>ESM_3</th><th>LMTD</th></tr>
<tr><td>1 parameter</td><td>1 parameter</td><td>1 parameter</td><td>4 parameters</td><td>2 parameters</td></tr>
<tr><td rowspan="3">$T_{out,p} = T_{in,s} + k_1$</td><td colspan="4">$T_{out,p} = \alpha T_{in,p} + (1-\alpha)T_{in,s}\ ,\quad 0 < \alpha < 1$</td></tr>
<tr><td rowspan="2">$\alpha = constant$</td><td rowspan="2">$\alpha = \frac{\dot{Q}}{UA(T_{in,p}-T_{in,s})}$, determined assuming $\dot{m}_s = \dot{m}_p$</td><td colspan="2">α determined with the LMTD method (20)</td></tr>
<tr><td>$\frac{\dot{m}_s}{\dot{m}_p} = f(\epsilon)$</td><td>Implicit formulation</td></tr>
</table>

2.6.2. Parameters identification

The parameters of these models are fitted using experimental data and relying on a least square regression method. Such a method has been programmed using the open source SCILAB software [22]. The program relies on the use of an optimization algorithm in charge of defining the combination of parameters that minimizes the root mean square (RMS) of the pairwise differences between the experimental and the numerical data sets. Since no weighting factor is considered, the RMS expression is defined as in (23) where n represents the total number of data.

$$RMS = \sqrt{\frac{1}{n}\sum_{i=1}^{n}\left(\left(T_{out,p}\right)_i^{exp} - \left(T_{out,p}\right)_i^{model}\right)^2} \qquad (23)$$

4 different substations datasets are considered in this study, namely SST_k with k from 1 to 4. Each substation is composed of a plate heat exchanger, a pressure independent regulation valve and an energy meter as shown in Fig. 1 a). The experimental datasets cover a time period of 11 months with a 15 minutes time step. Data with no heat demand are excluded from the original datasets since they are useless for the model error analysis and sometime results in convergence difficulties during simulation. We have considered only one of two values in the identification process, the rest of the data being used for the validation phase (cf. paragraph below).

2.6.3. Validation

The accuracy of the models is assessed using the remaining 50 % experimental data that were not used in the parameter identification procedure. The error of the models is evaluated through the primary outlet temperature $T_{out,p}$ using the absolute error and the Mean Absolute Error (MAE) (see (24)) between the experimental and simulated results.

$$MAE = \frac{1}{n}\sum_{i=1}^{n}\left|\left(T_{out,p}\right)_i^{exp} - \left(T_{out,p}\right)_i^{model}\right| \qquad (24)$$

In Fig. 2, the monthly and global MAE are reported for each substation and each model. Figure 3 depicts the absolute error histogram for each substation. The black dotted lines represent the experimental uncertainty of the temperature measurements.

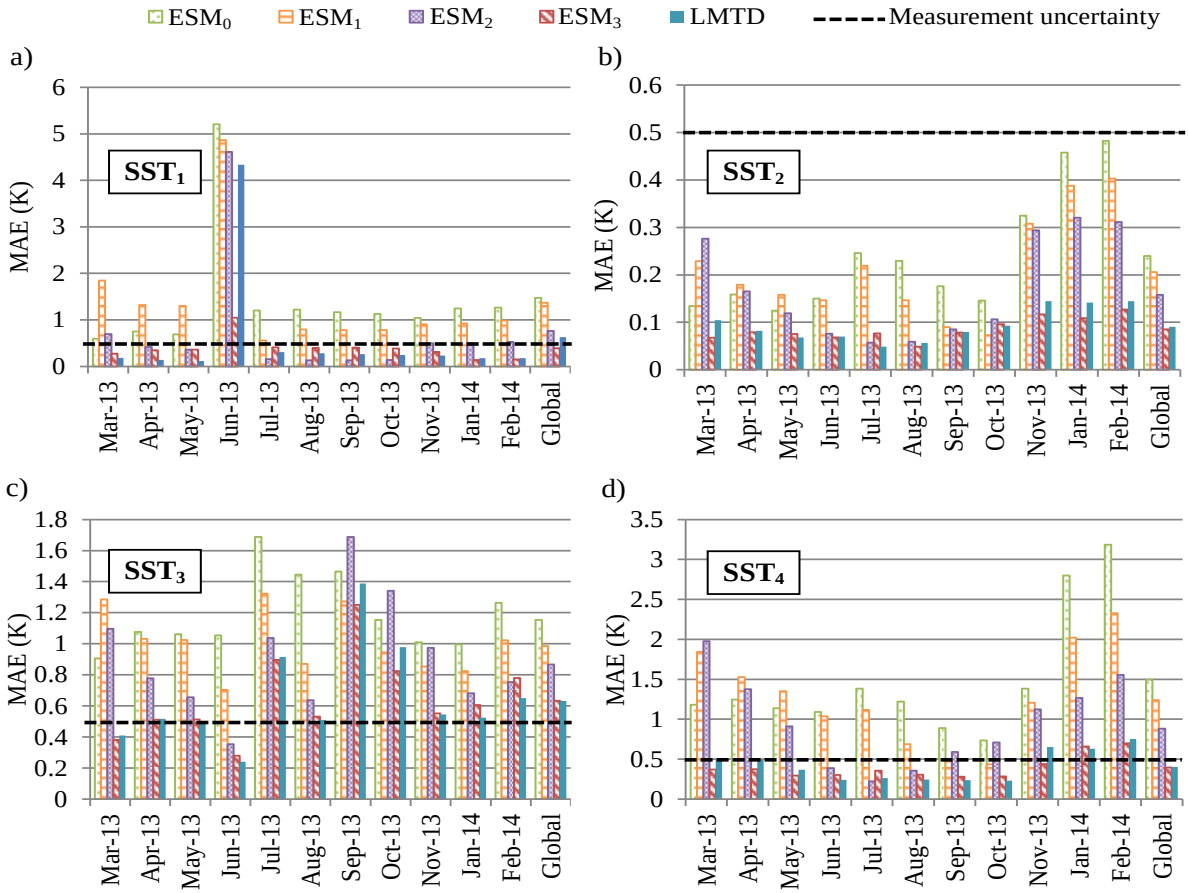

Fig. 2. Monthly Mean absolute error for each substation: a) SST1, b) SST2, c) SST3 and d) SST4

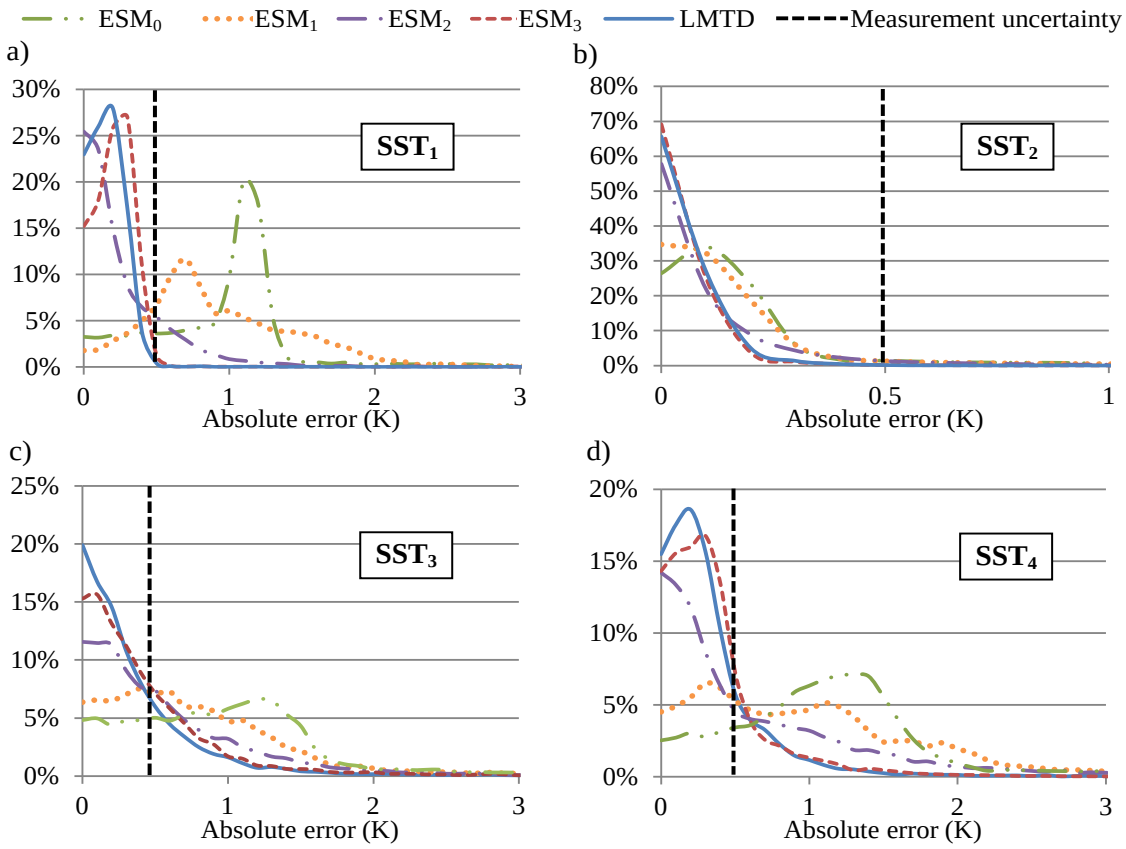

Fig. 3. Histogram of absolute error for each substation: a) SST1, b) SST2, c) SST3 and d) SST4

In SST_1 (cf. Fig. 2 a)), we note that for each model, the MAE in June is higher than for the other months. By analyzing the temperature evolutions at that period (not shown here) we have concluded that this is most probably due to exceptional maintenance operations not considered in our models.

Figures 2 and 3 show that, among the one parameter models, namely ESM_i with i from 0 to 2, ESM_2 is the most accurate for each of the 4 tested substations. It can be concluded that though very simplified, the physical bases that support the ESM_2 model enhance the quality of the temperature prediction. However, accuracy can still be improved as shown in Figs 2 and 3 with the use of the ESM_3 and LMTD models which yield similar results. Indeed, both have comparable MAE and their error histograms are relatively close and mostly centered on 0. For instance, the global ESM_3 MAE ranges between 0.6 % (for SST_2) and 4.9 % (for SST_1) of the primary temperature difference. This is consistent with the fact that both models entirely rely or are very close to the LMTD theoretical formulation (see [20]). However, due to its explicit nature, the ESM_3 model is much more computationally efficient than the LMTD model. It is also interesting to compare the present models to those reported previously by other research groups, e.g. the five parameters Tr5 model by Benonysson [3]. The same calculations as those previously presented have been conducted for the Tr5 model. From these additional computations it can be concluded that in the operational conditions evaluated in the present study, the accuracy of the Tr5 model is comparable to that of the ESM_2 model. In conclusion, the ESM_3 model represents the best compromise between accuracy and numerical performances for our application.

3. Global simulation, results and discussion

3.1. The Grenoble case study

The city of Grenoble comprises 400,000 inhabitants and is equipped with the second largest district heating net in France. This district heating system is operated by the CCIAG company. The net is composed of 160 km of meshed pipes, 3 heat production units and delivers heat to approximately 1000 substations. The annual energy amount distributed by the network is close to 900 GWh. Our group is currently involved in a joint research program with CCIAG devoted to the optimization of the existing control strategies. As a first step, it is decided here to evaluate different control strategies for the supply temperature on a smaller virtual district heating system. This virtual network is composed of 26 substations, 1 circulation pump and a 30 thermal MW heat only boiler.

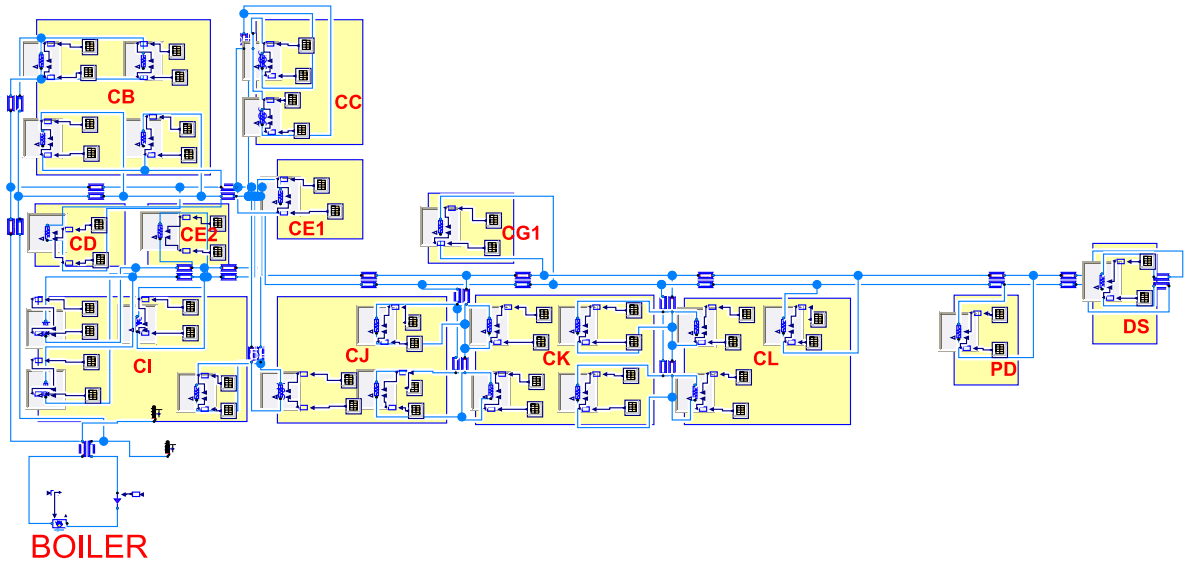

Fig. 4. The virtual district heating model within the MODELICA/DYMOLA simulation platform

The mesh-free network layout considered in the virtual network originates from an extension project of the main Grenoble district heating net (see Fig. 4). The hourly heat load profiles used to simulate the consumers come from the historical database of CCIAG. In France, district heating

clients are composed of 58 % of households, 36% of services and 6 % of industries. The substation models have been dimensioned according to the local rules stating that the dimensioning load must be deliverable to consumers at a pressure difference of 1 bar and a heat exchanger temperature difference of 110 K (i.e. $T_{in,p} - T_{in,s} = 110$ K) .

Pipes internal diameters were chosen within the range DN65 to DN350 in order to limit the maximal fluid velocity to 1.5 m/s. This leads to a maximum heat transportation time between the boiler and the far end consumer of 3 hours in the operating conditions investigated in the present work. The global heat losses coefficient of the network was adjusted to limit the relative losses to 10 % of the distributed energy during typical winter days.

3.2. Results

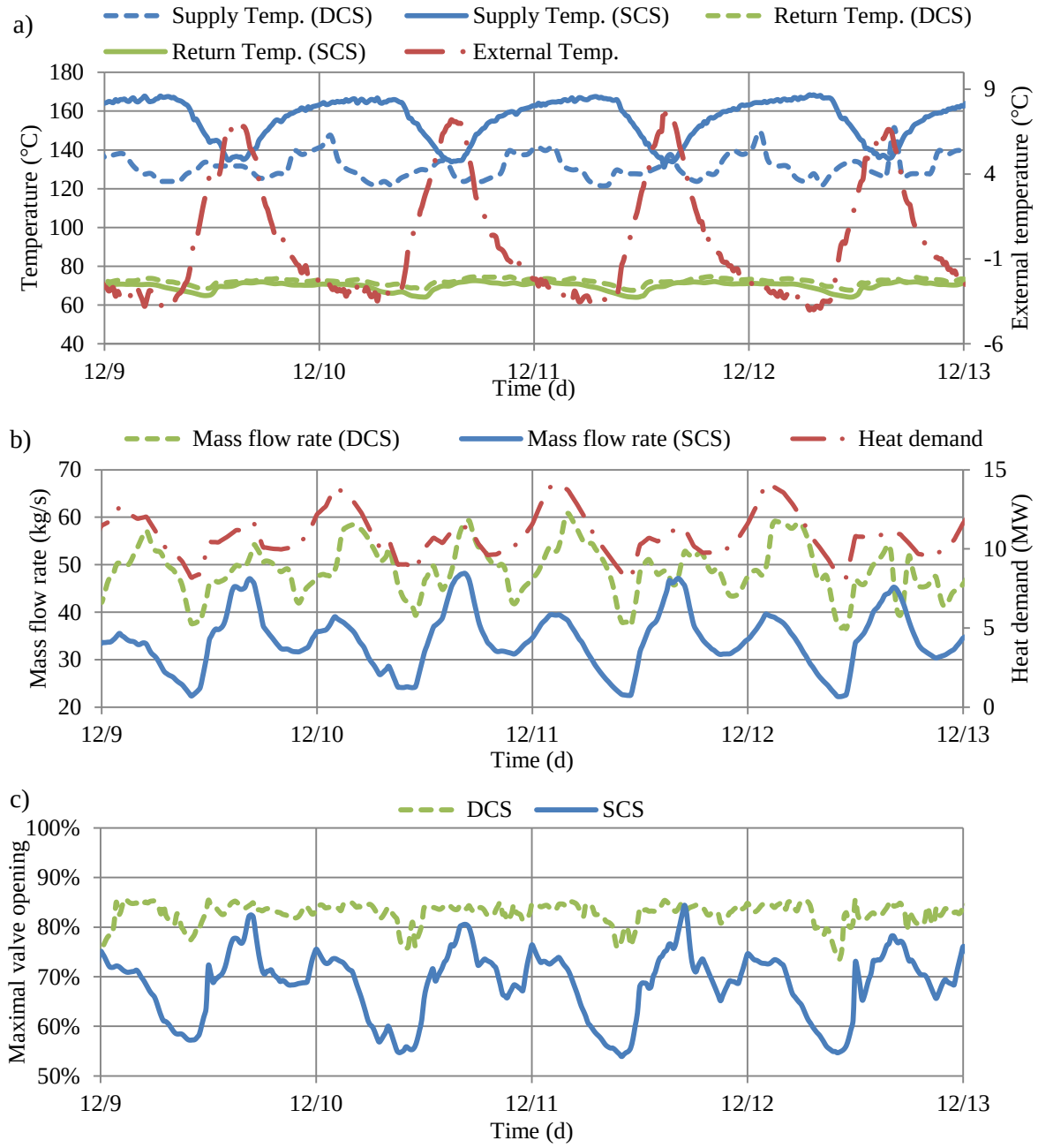

Fig. 5. Comparison of the two control strategies: a) supply, return and external temperatures, b) mass flow rates and total heat demand and c) maximal valve opening

The simulation period covers five consecutive days of December 2013 characterized by a cold yet sunny anticyclonic weather with daily temperature variations ranging between – 4.1 °C and + 8.1

°C. Two simulations respectively relying on a static heating curve and a dynamic supply temperature algorithm have been conducted. In the first simulation, namely SCS (for Static Control Strategy), the supply temperature at the boiler is chosen as a linear function of the external temperature, as can be seen in Fig. 5 a). The linear dependency between the supply and external temperatures is adapted so that the maximal valve opening of the 26 consumers never exceeds 85 % during the simulation period. In the second simulation, namely DCS (for Dynamic Control Strategy), the supply temperature planning is chosen in such a way that the maximal valve opening of the 26 consumers always remain close to 85 %. For both simulations, the pressure difference between the supply and return networks is fixed at 5 bars at the production plant. Each simulation covering the five days winter period lasts 20 s on a DELL laptop equipped with an Intel Core i5 2.6 GHz processor.

Figure 5 a) shows the evolutions of the supply and return temperatures for both control strategies and the external temperature. As can be seen, the DCS strategy leads to lower supply, to higher mass flow-rates (see Fig. 5 b)) and also to higher maximal valve opening (see Fig. 5 c)) while there is no significant change on the return temperature. As a consequence, the DCS strategy leads to global thermal energy savings of 10 % (- 11 MWh) of the thermal distribution losses with an increase of + 24 % (+0.56 MWh_{el}) of the pumping energy. All in all, since the ratio of electrical to thermal energy prices is of the order of three, the DCS control strategy both decreases distribution losses and costs.

Figure 5 b) presents the total heat power demand on the simulated period. This evolution is similar to the DCS strategy supply temperature (see Fig. 5 a)) since this strategy accounts for the dynamic heat demand variations. However, there is a time delay between the 2 curves corresponding to the heat transportation time. For instance, the 12/10 heat demand peak occurs approximately at 2:30 a.m., i.e. 90 minutes after the supply temperature peak. This delay corresponds to the time necessary to transport the heat to the most critical substation.

4. Conclusion

In this paper we proposed a physical model for simulating district heating networks and successfully applied it to a virtual district heating system built to be a very simplified version of the Grenoble district heating net. Both hydraulic and thermal models were derived in a mathematical form that allows accurate predictions at low computational costs. The model is able to predict temperature and flows anywhere in the system. Thus it can serve as a basis to the evaluation of different control strategies. We evaluated two supply temperature control strategies on the virtual test bed and showed that applying a dynamic supply temperature algorithm reduces the distribution losses by an amount of 10 % when compared to a fixed heating curve only based on the outdoor temperature. In both cases, the pumping energy remains low and represents at most 2 % of the distribution losses.

Future work will be devoted to the automation of the dynamic control strategy algorithm. We will also focus our efforts on scaling up our developments in order to be able to implement and test them on the district heating of Grenoble.

Acknowledgments

The authors wish to thank Elise Le Goff, Nicolas Giraud and Philippe Clolot from CCIAG for their fruitful help in the realization of this study. We also would like to acknowledge the financial support of CCIAG for the joint research program and of ADEME for the PhD of Loïc GIRAUD.

Nomenclature

A Section, m^2

b Parameter of the ESM_3 model

c Parameter of the ESM_3 model

c_p Specific heat capacity, J.kg^{-1}.K^{-1}

C' Heat capacity of the production plant, J.K^{-1}

D Pipe diameter, m

f Fanning friction factor

h Enthalpy, J.kg^{-1}

K Linear global heat transfer coefficient, W.m^{-1}.K^{-1}

k Coefficient used to determine the global heat transfer coefficient UA, J.kg^{-1}.K^{-1}

k_1 Parameter of the ESM_0 model

L Pipe length, m

$\dot{m}$ Mass flow rate, kg.s^{-1}

MAE Mean Absolute Error, K

n Number of data

P Pressure, Pa

ΔP Pressure difference, Pa

q Parameter used to determine the global heat transfer coefficient UA

$\dot{Q}$ Heat, W

$\dot{Q}_{losses}$ Heat losses, W

RMS Root Mean Square, K

S Source term in the energy balance, W

t Time, s

T Temperature, K

T^* Temperature without taking into account the tube heat capacity, K

ΔT Temperature difference, K

ΔT_{err} Heat only boiler parameter, K

UA Global heat transfer coefficient, W.K^{-1}

v Velocity, m.s^{-1}

V Volume, m^3

x Position, m

4.1.1.1. Greek symbols

α Coefficient used in the substation models

ρ Density, kg.m^{-3}

ϵ Efficiency of a substation, used in the ESM_3 model

τ Heat transportation time, s

4.1.1.2. Subscripts

$_a$ Tube

$_{ext}$ External

$_f$ Fluid

$_{in}$ Inlet

$_{nom}$ Nominal

$_{out}$ Outlet

$_p$ Primary side of the substations

$_s$ Secondary side of the substations

$_{set}$ Set point

References

[1] Euroheat and Power. District Heating and Cooling Country by Country Survey. 2013.

[2] Direction Générale de l'Energie et du Climat. Programmation pluriannuelle des investissements de production de chaleur - Période 2009- 2020. 2009 p. 114.

[3] Benonysson A. Dynamic Modelling and Operational Optimization of District Heating Systems. [Lyngby, Denmark]: Technical University of Denmark; 1991.

[4] Zhao H. Analysis, modelling and operational optimization of district heating systems. [Lyngby, Denmark]: Technical University of Denmark; 1995.

[5] Palsson H. Methods for Planning and Operating Decentralized Combined Heat and Power Plants. [Roskilde, Denmark]: Technical University of Denmark; 2000.

[6] Sandou G. Modélisation, Optimisation et commande de parcs de production multi-énergies complexes [Science Appliquée]. [Paris, France]: Université Paris XI Orsay; 2006.

[7] Ben Hassine I, Eicker U. Simulation and optimization of the district heating network in Scharnhauser Park. Proceedings of the 2nd Polygeneration Conference. Tarragona, Spain: Salcedo AC; 2011.

[8] Grosswindhager S, Voigt A, Kozek M. Efficient Physical Modelling Of District Heating Networks. Proceedings of the 22nd IASTED International Symposia on Modelling and Simulation. Calgary, Canada: M.H. Hamza; 2011.

[9] Velut S, Larsson PO, Saarinen L, Boman K, Windahl J. Short-term production planning for district heating networks with JModelica. Proceedings of the 10th International Modelica Conference. Lund, Sweden: Hubertus Tummescheit and Karl-Erik Årzén; 2014.

[10] Giraud L, Bavière R, Paulus C. Modeling of Solar District Heating: A Comparison between TRNSYS and Modelica. Proceedings of EuroSun 2014. Aix-les-Bains, France; 2014.

[11] Modelica Association. Modelica - Language specification - Version 3.3. 2012.

[12] Dassault Systèmes. Dymola User manual - Volume 1. 2013. 558 p.

[13] Dassault Systèmes. Dymola User Manual - Volume 2. 2013. 384 p.

[14] Swamee PK, Jain AK. Explicit equations for pipe-flow problems. J Hydraul Div ASCE. 1976;102(5):657–64.

[15] Johnson RS. First order partial differential equations. School of Mathematics & Statistics - University of Newcastle; 2010.

[16] Gabrielaitiene I, Bøhm B, Sunden B. Evaluation of Approaches for Modeling Temperature Wave Propagation in District Heating Pipelines. Heat Transf Eng. 2008;29(1):45–56.

[17] Čiuprinskas K, Narbutis B. Experiments on heat losses from district heating pipelines. Energetika. 1999;(2):35–40.

[18] ISA Standards. Flow Equations for Sizing Control Valves - ISA-75.01.01.2007. Standard; 2007.

[19] Schneider Electric. Termis, User Guide Version 5.0. 2012.

[20] Shah RK, Sekulić DP. Fundamentals of heat exchanger design. Wiley; 2003.

[21] Larsen HV, Pálsson H, Bøhm B, Ravn HF. Equivalent Models for District Heating Systems. Proceedings of the 7th International Symposium on District Heating and Cooling. Lund, Sweden: S. Frederiksen; 1999. p. 1–16.

[22] Scilab Enterprises. Scilab: Free and Open Source software for numerical computation [Internet]. 2012 [cited 2014 Oct 12]. Available from: http://www.scilab.org